

Vector dark energy and high- z massive clusters

Edoardo Carlesi,^{1*} Alexander Knebe,¹ Gustavo Yepes,¹ Stefan Gottlöber,³
Jose Beltrán Jiménez,^{4,5} Antonio L. Maroto,²

¹*Departamento de Física Teórica, Universidad Autónoma de Madrid, 28049, Cantoblanco, Madrid, Spain*

²*Departamento de Física Teórica, Universidad Complutense de Madrid, 28040, Madrid, Spain*

³*Leibniz Institut für Astrophysik, An der Sternwarte 16, 14482, Potsdam, Germany*

⁴*Institute de Physique Théorique, Université de Genève, 24 quai E. Ansermet, 1211 Genève, Switzerland*

⁵*Institute of Theoretical Astrophysics, University of Oslo, 0315 Oslo, Norway*

Accepted XXXX . Received XXXX; in original form XXXX

ABSTRACT

The detection of extremely massive clusters at $z > 1$ such as SPT-CL J0546-5345, SPT-CL J2106-5844, and XMMU J2235.3-2557 has been considered by some authors as a challenge to the standard Λ CDM cosmology. In fact, assuming Gaussian initial conditions, the theoretical expectation of detecting such objects is as low as $\leq 1\%$. In this *Letter* we discuss the probability of the existence of such objects in the light of the Vector Dark Energy (VDE) paradigm, showing by means of a series of N -body simulations that chances of detection are substantially enhanced in this non-standard framework.

Key words: methods: N -body simulations – galaxies: haloes – cosmology: theory – dark matter

1 INTRODUCTION

Present day cosmology is still failing to explain satisfactorily the nature of dark energy, which is supposed to dominate the energetic content of the universe today and to be responsible for the current accelerated expansion. In the standard Λ CDM model, this cosmic acceleration is generated by the presence of a cosmological constant. However, the required value for that constant turns out to be tiny when compared to the natural scale of gravity, namely the Planck scale. Thus, the gravitational interaction would hence be described by two dimensional constants differing by many orders of magnitude, and this poses a problem of naturalness. This is the so-called “cosmological constant problem” and it motivated to consider alternative explanations for the current acceleration of the universe by either modifying the gravitational interaction at large distances or introducing a new dynamical field.

Indeed, one of the main challenges of observational cosmology is exactly to devise new tests which could help discriminating between the constant or dynamic nature of dark energy. In this regard, several authors have recently pointed out that the observation of extremely massive clusters at high redshift, such as SPT-CL J2106-5844 (Foley et al. (2011), $z \simeq 1.18$, $M_{200} = (1.27 \pm 0.21) \times 10^{15} M_{\odot}$), SPT-CL J0546-5346 (Brodwin et al. (2010), $z \simeq 1.07$, $M_{200} = (7.95 \pm 0.92) \times 10^{14} M_{\odot}$), and XMMU J2235.3-2557 (Jee et al. (2009), $z \simeq 1.4$, $M_{200} = (7.3 \pm 1.3) \times 10^{14} M_{\odot}$) may represent a major shortcoming of the Λ CDM paradigm, where the presence of such objects should be in principle strongly disfavoured

(see, for example, Baldi & Pettorino 2011; Mortonson et al. 2011). While, on the one hand, this tension could be solved keeping the standard scenario and relaxing the assumption of Gaussianity in the initial conditions (as proposed in Hoyle et al. (2011) and Enqvist et al. (2011)), it could be as well possible to use this observations as a constraint for different cosmological models. In this work we look at the VDE model, where the role of the dark energy is played by a cosmic vector field (Beltrán Jiménez & Maroto 2008). By means of a series of N -body simulations, we study the large scale clustering properties of this cosmology, computing the cumulative halo mass functions at different redshifts and comparing them to the predictions of the standard model. In this way, we are able to show that the VDE cosmology does indeed predict a higher abundance of massive haloes at all redshifts, thus enhancing the probability of observing such objects with respect to Λ CDM.

2 VECTOR DARK ENERGY

The action of the vector dark energy model (see Beltrán Jiménez & Maroto (2008)) can be written as:

$$S = \int d^4x \sqrt{-g} \left[-\frac{R}{16\pi G} - \frac{1}{4} F_{\mu\nu} F^{\mu\nu} - \frac{1}{2} (\nabla_{\mu} A^{\mu})^2 + R_{\mu\nu} A^{\mu} A^{\nu} \right]. \quad (1)$$

where $R_{\mu\nu}$ is the Ricci tensor, $R = g^{\mu\nu} R_{\mu\nu}$ the scalar curvature and $F_{\mu\nu} = \partial_{\mu} A_{\nu} - \partial_{\nu} A_{\mu}$. This action can be interpreted as the Maxwell term for a vector field supplemented with a gauge-fixing

* E-mail: edoardo.carlesi@uam.es

term and an effective mass provided by the Ricci tensor. It is interesting to note that the vector sector has no free parameters nor potential terms, being G the only dimensional constant of the theory.

For a homogeneous and isotropic universe described by the flat Friedmann-Lemaître-Robertson-Walker metric:

$$ds^2 = dt^2 - a(t)^2 d\vec{x}^2 \quad (2)$$

we have $A_\mu = (A_0(t), 0, 0, 0)$ so that the corresponding equations read:

$$\ddot{A}_0 + 3H\dot{A}_0 - 3 \left[2H^2 + \dot{H} \right] A_0 = 0 \quad (3)$$

$$H^2 = \frac{8\pi G}{3} [\rho_R + \rho_M + \rho_A] \quad (4)$$

with $H = \dot{a}/a$ the Hubble parameter and:

$$\rho_A = \frac{3}{2}H^2 A_0^2 + 3H A_0 \dot{A}_0 - \frac{1}{2}\dot{A}_0^2 \quad (5)$$

the energy density associated to the vector field, while ρ_M and ρ_R are the matter and radiation densities. During the radiation and matter eras in which the dark energy contribution was negligible, we can solve Eq. (3) with $H = p/t$, where $p = 1/2$ for radiation and $p = 2/3$ for matter eras respectively, that is equivalent to assume that $a \propto t^p$. In that case, the general solution is:

$$A_0(t) = A_0^+ t^{\alpha_+} + A_0^- t^{\alpha_-}, \quad (6)$$

with A_0^\pm constants of integration and $\alpha_\pm = -(1 \pm 1)/4$ in the radiation era, and $\alpha_\pm = (-3 \pm \sqrt{33})/6$ in the matter era. After dark energy starts dominating, the equation of state abruptly falls towards $w_{DE} \rightarrow -\infty$ as the Universe approaches t_{end} , and the equation of state can cross the so-called phantom divide line (Nesseris & Perivolaropoulos (2007)), so that we can have $w_{DE}(z=0) < -1$.

Using the growing mode solution in (6) we can obtain the evolution for the energy density as:

$$\rho_A = \rho_{A0}(1+z)^\kappa, \quad (7)$$

with $\kappa = 4$ in the radiation era and $\kappa = (9 - \sqrt{33})/2 \simeq -1.63$ in the matter era. Thus, the energy density of the vector field scales like radiation at early times so that the ratio ρ_A/ρ_R is constant during such a period. Moreover, the value of the vector field A_0 during that era is also constant hence making the cosmological evolution insensitive to the time at which we impose the initial conditions (as long as they are set well inside the radiation dominated epoch). Also, such constant values are $\rho_A/\rho_R|_{\text{early}} \simeq 10^{-6}$ and $A_0^{\text{early}} \simeq 10^{-4} M_p$ which are values that can arise naturally during the early universe, for instance, as quantum fluctuations. Furthermore, they do not need the introduction of any unnatural scale, thus, alleviating the naturalness or coincidence problem. On the other hand, when the Universe enters the era of matter domination, ρ_A starts growing relative to ρ_M eventually overcoming it at some point so that the dark energy vector field becomes the dominant component.

Once the present value of the Hubble parameter H_0 and the constant A_0^{early} during radiation (which fixes the total amount of matter Ω_M) are specified, the model is completely determined. In other words, this model contains the same number of parameters as Λ CDM, i.e. the minimum number of parameters of any cosmological model with dark energy. Notice however, that in the VDE model the present value of the equation of state parameter

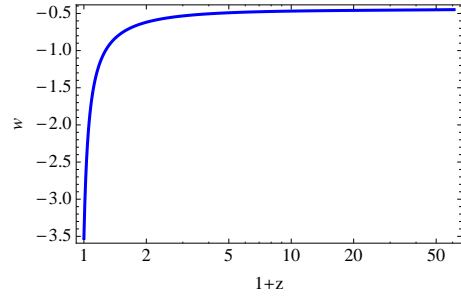


Figure 1. Equation of state of the vector dark energy model for the best fit to SNIa data.

$w_0 = -3.53$ is radically different from that of a cosmological constant (cf. Fig. 1, where the redshift evolution of $\omega(z)$ is shown over the range of our simulations). Despite this fact, VDE is able to fit supernovae and CMB data with comparable goodness to Λ CDM (Beltrán Jiménez & Maroto 2008; Beltrán Jiménez et al. 2009).

3 THE DATA

3.1 Simulations

We wanted to estimate the probability of finding massive clusters at $z > 1$ in the VDE scenario compared to the Λ CDM one by means of CDM only N -body simulations. For this purpose, we chose to use a suitably modified version of the publicly available GADGET-2 tree-PM code (Springel 2005), which had to take into account the different expansion history that characterizes the two cosmologies. In Table 1 we show the cosmological parameters used in the different simulations. For the VDE model, we have used the value of Ω_M provided by the best fit SNIa and then we have fitted WMAP7 in order to obtain the remaining cosmological parameters. w_0 denotes the present value of the equation of state parameter of dark energy. For Λ CDM we used the Multidark Simulation (Prada et al. 2011) cosmological parameters with a WMAP7 σ_8 normalization (Larson et al. 2011). We also introduced a so called Λ CDM-vde model, which is a standard Λ CDM one implementing the same Ω_M and σ_8 as VDE. Although this cosmology is non-viable and ruled out by experimental data, its study allows us to disentangle and highlight the effect of the increased matter density and of matter perturbations normalization on our findings.

We chose to run a total of eight 512^3 particles simulations summarized in Table 2 and explained below:

- a VDE (and a Λ CDM started with the same seed for the phases of the initial conditions) simulation in a $500 h^{-1}$ Mpc box,
- a second VDE (and again corresponding Λ CDM) simulation in a $1 h^{-1}$ Gpc box,
- two more VDE simulations with a different random seed, one in a $500 h^{-1}$ Mpc and one in a $1 h^{-1}$ Gpc box, as a check for the influence of cosmic variance,
- two Λ CDM-vde simulations in a $500 h^{-1}$ Mpc and a $1000 h^{-1}$ Mpc box.

The full set of simulations will be presented and analyzed in an upcoming companion paper; in this work, instead, we chose to focus on some of them only in order to gather information on large scale clustering in the two cosmologies. The use of the same initial seed in the coupled Λ CDM-VDE simulations allows us to directly

Table 1. Cosmological parameters for Λ CDM Λ CDM-vde and VDE.

Model	Ω_m	Ω_{de}	w_0	σ_8	h
Λ CDM	0.27	0.73	-1	0.8	0.7
Λ CDM-vde	0.388	0.612	-1	0.83	0.7
VDE	0.388	0.612	-3.53	0.83	0.62

Table 2. N -body settings used for the GADGET-2 simulations, the two $500h^{-1}$ Mpc and the two $1h^{-1}$ Gpc have the same initial random seed and starting redshift $z_{\text{start}} = 60$ in order to allow for a direct comparison of the halo properties. The number of particles in each was fixed at 512^3 . The box size B is given in $h^{-1}M_\odot$ and the particle mass in $h^{-1}M_\odot$. The cosmology refers back to the parameters listed in Table 1.

Simulation	B	m_p
2×VDE-0.5	500	1.00×10^{11}
2×VDE-1	1000	8.02×10^{11}
Λ CDM-0.5	500	6.95×10^{10}
Λ CDM-1	1000	5.55×10^{11}
Λ CDM-0.5vde	500	1.00×10^{11}
Λ CDM-1vde	1000	8.02×10^{11}

compare the structures identified by the halo finder, which are supposed to form at the same points corresponding to the overdensity peaks formed from the initial Gaussian density field.

As a final remark, we underline here that the choice of the boxes was made in order to allow the study of clustering on larger scales, without particular emphasis on the low mass results, e.g. objects with $M < 10^{14}h^{-1}M_\odot$. This means that even though our halo finder has been able to identify objects down to $\sim 10^{12}h^{-1}M_\odot$ in the $500h^{-1}$ Mpc box and $\sim 10^{13}h^{-1}M_\odot$ in the $1h^{-1}$ Gpc one (which correspond to a lower limit of 20 particles), we are not comparing the mass spectrum at this far end. Therefore, since we are only interested in studying the behaviour of the mass function of these models at the very high mass end, in the following section we will refer mostly to the Λ CDM-1, Λ CDM-vde and VDE-1 simulations, where we have a larger statistics for the supercluster scales.

3.2 Halo Finding

In order to identify halos in our simulation we have run the MPI+OpenMP hybrid halo finder AHF¹ described in detail in Knollmann & Knebe (2009). AHF is an improvement of the MHF halo finder (Gill et al. 2004), which locates local overdensities in an adaptively smoothed density field as prospective halo centres. The local potential minima are computed for each of these density peaks and the gravitationally bound particles are determined. Only peaks with at least 20 bound particles are considered as haloes and retained for further analysis, even though here we focus on the most massive objects only.

The mass of each halo is then computed via the equation

$$M(r) = \frac{4\pi}{3} \Delta \rho_c r^3 \quad (8)$$

¹ AMIGA halo finder, to be downloaded freely from <http://www.popia.ft.uam.es/AMIGA>

where we applied $\Delta = 200$ as the overdensity threshold. Using this relation, particular care has to be taken when considering the definition of the critical density

$$\rho_c = \frac{3H^2}{8\pi G} \quad (9)$$

because it involves the Hubble parameter, that differs substantially at all redshifts in the two models. This means that, identifying the halo masses, we have to take into account the fact that the value of ρ_c changes from Λ CDM and VDE. This has been incorporated into and taken care of in the latest version of AHF where $H_{VDE}(z)$ is being read in from a precomputed table.

We would like to mention that we checked that the objects obtained by this (virial) definition are in fact in equilibrium. To this extent we studied the ratio between two times kinetic over potential energy $2T/|U|$ confirming that at each redshift under investigation here this relation is equally well fulfilled for the Λ CDM and – more importantly – the VDE simulations. We therefore conclude that our adopted method to define halo mass in the VDE model leads to unbiased results.

4 THE RESULTS

4.1 Mass Function

With the halo catalogues at our disposal, we computed the cumulative mass functions $n(> M)$ at various redshifts. We show in Fig. 2 the results for the $1h^{-1}$ Gpc simulations at redshifts $z = 1.4$, $z = 1.2$, $z = 1.1$ and $z = 0$. This plot is accompanied by Table 3 where we list the masses of the most massive haloes found in each model and the redshifts under consideration.

We notice that the mass function for $M > 10^{14}h^{-1}M_\odot$ is several times larger in VDE than in Λ CDM at all redshifts, thus increasing significantly the number of higher mass haloes in this non-standard cosmological model. In particular, at the high-mass end the VDE mass function is about three times larger at the relevant redshifts $z = 1.4$, 1.2 , and 1.1 – and even larger at today's time.

In order to verify that this feature of the VDE model is not a simple reflection of cosmic variance (which should affect in particular the high mass end, where the statistics is smaller) we compared the results presented in Fig. 2 to the mass functions of the set of two additional simulations started from a different random seed for the initial conditions. In fact, the VDE cumulative mass function turns out to outnumber the Λ CDM one by the same factor at all redshifts in these two test runs, too.

An interesting remark we would like to add here, is that the physical mass (obtained dividing by the corresponding h values the values quoted in $h^{-1}M_\odot$ units) of the largest haloes in the VDE-1 simulation at $z = 1.4$, $z = 1.2$ and $z = 1.1$ are perfectly compatible with the ones of the above cited clusters, whereas the corresponding Λ CDM candidates are outside the 2σ compatibility level. And again, similar massive clusters have also been found in the duplicate VDE-1 simulation with a different initial seed.

As an additional note, we observe that the Λ CDM-1vde simulations yields a mass function is almost indistinguishable from the VDE one for $M < 10^{14} \times h^{-1}M_\odot$ whereas it is a factor of ~ 3 higher than the VDE one in the high mass range. This is a clear indication that the higher normalization of the matter fluctuations and, most important, the higher value of Ω_M act as the main sources of the enhancement of clustering found in VDE-1 and VDE-0.5. On

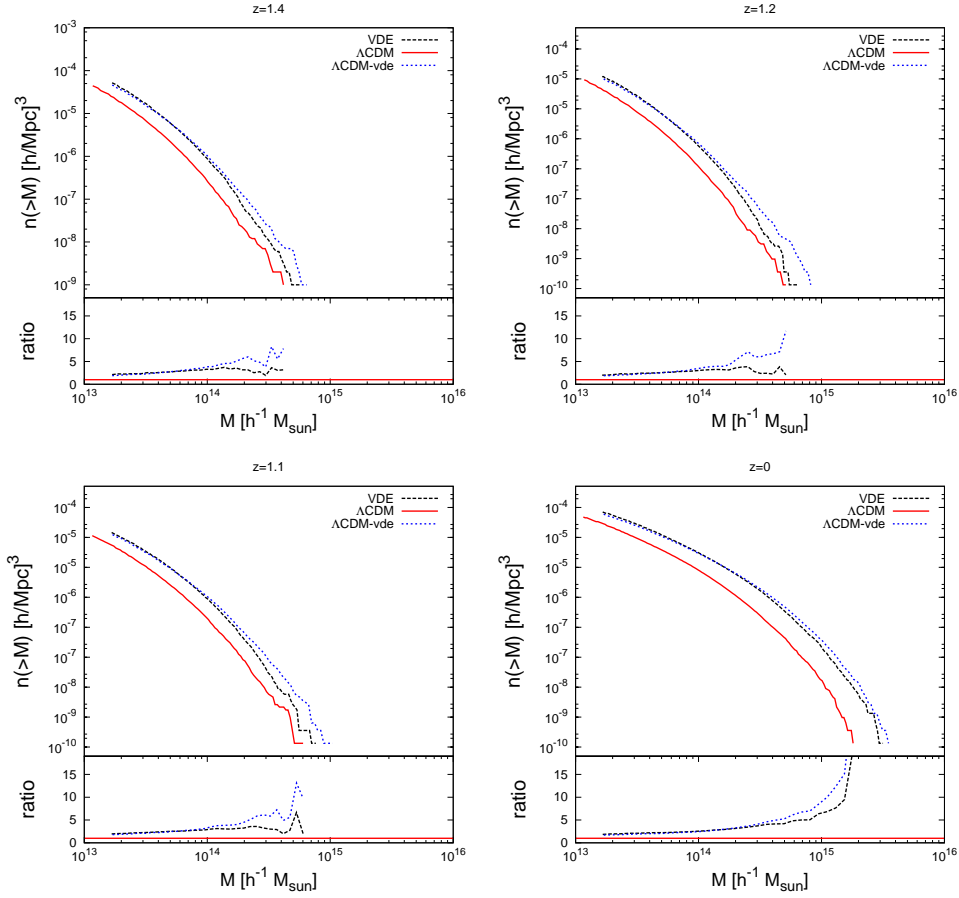


Figure 2. Mass functions (and their ratios) as computed for the VDE-1, Λ CDM-1 and Λ CDM-1vde simulations at $z = 1.4, 1.2, 1.1,$ and 0 . These redshifts have been chosen in order to overlap with the aforementioned observed massive clusters.

Table 3. The most massive halo found in the three $1h^{-1}\text{Gpc}$ simulations (in units of $10^{14}h^{-1}M_{\odot}$) as a function of redshift.

z	Λ CDM-1	VDE-1	Λ CDM-1vde
1.4	4.16	5.63	6.47
1.2	5.13	6.51	8.16
1.1	6.01	7.63	10.2
0	18.1	31.6	35.1

the one hand, this complicates the issue of model selection, since (although disfavoured by the WMAP7 data) we could invoke a bigger Ω_M or a higher σ_8 normalization at $z = 0$ for Λ CDM to explain the current tension with the high- z massive clusters observations. On the other hand, the distinct expansion history that characterizes and differentiates between the two Λ CDM and VDE models would still leave a clear imprint on structure formation at different times, which could be detected e.g. measuring σ_8 's dependence on the redshift. Such a test would indeed provide invaluable information for the study of Λ CDM and for any cosmological model beyond it such as VDE.

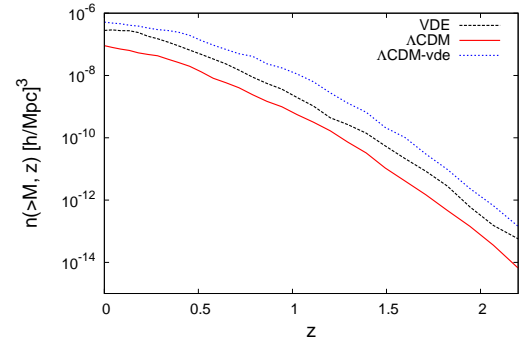


Figure 3. Theoretical cumulative number densities of objects with $M > 5 \times 10^{14}M_{\odot}$ for VDE and Λ CDM.

4.2 Probability

In order to provide a more quantitative estimate of the the relative probability of observationally detecting such massive clusters we used $n(> M, z)$ – the expected cumulative number density of objects above a threshold mass M as a function of redshift as given by our simulations – and integrated it over the comoving volume V_c of the survey

Table 4. Expected number of objects $N(> M)$ in excess of mass M and inside a certain (comoving) volume in the Λ CDM and VDE for different mass thresholds and survey volumes. Solid angles Ω are measured in deg^2 and masses are measured in $10^{14} h^{-1} M_{\odot}$.

M	Δz	Ω_{survey}	$N_{\Lambda\text{CDM}}$	N_{VDE}	$N_{\Lambda\text{-VDE}}$
> 10	> 1	2500	0.007	0.02	0.04
> 7	> 1	2500	0.03	0.31	0.56
> 5	1.38 – 2.2	11	0.005	0.06	0.07

$$N(> M) = \int_{\Delta z, \Omega_{\text{survey}}} n(> M, z) dV_c(z) \quad (10)$$

where Δz and Ω_{survey} are the redshift interval and the fraction of the sky covered by the survey to which we want to compare our theoretical expectations.

While $n(> M, z)$ can be readily calculated in Λ CDM cosmologies (e.g. Press & Schechter 1974; Sheth & Tormen 1999; Jenkins et al. 2001; Tinker et al. 2008), in VDE we have to devise a strategy to compute it based upon our numerical results only by adjusting the formula of Sheth & Tormen (1999):

- we calculated the cumulative number densities in the desired redshift intervals Δz based upon our simulation data,
- we adjusted the parameters of the Sheth-Tormen mass function fitting the numerical cumulative number densities derived from the VDE-1 and VDE-0.5 simulations,
- we used these best fit estimates to analytically compute $n(> M, z)$ now having access to masses outside our numerically limited range to be used with Eq. (10).

The results of the numerical integration over the comoving volumes (obtained using the limits quoted in the observational papers by Jee et al. (2009), Brodwin et al. (2010) and Foley et al. (2011)) are listed in Table 4 for the VDE, Λ CDM-vde and Λ CDM model. We can clearly see that the chances are substantially larger to find such massive objects as the ones observed by Jee et al. (2009), Brodwin et al. (2010) and Foley et al. (2011) in VDE than in Λ CDM. We complement these results with Fig. 3 where we plot the abundance evolution of clusters with mass $M > 5 \times 10^{14} h^{-1} M_{\odot}$ computed with above described procedure. This plot confirms our previous analysis of the mass functions and shows that the expectation of massive objects is enhanced in VDE by a factor ~ 3 to ~ 10 at all redshifts, a factor which is even higher for Λ CDM-vde. We would like to remark here that while our Λ CDM estimate for the third cluster is in agreement with the result quoted by Jee et al. (2009) (obtained using our same approach), the same calculation done for the first one leads to an estimate substantially smaller than the one quoted by Foley et al. (2011), calculated using a Monte Carlo technique. However, this does not affect our conclusions, which are based on the comparison of results obtained in a consistent manner for the two models.

5 CONCLUSIONS

The observation of massive clusters at $z > 1$ provides an additional, useful test for Λ CDM and other cosmological models beyond the standard paradigm. In this *Letter* we have shown that the

Vector Dark Energy (VDE) scenario (Beltrán Jiménez & Maroto 2008) might account for such observations better than the Λ CDM concordance model, since the relative abundance of extremely massive cluster is at all redshifts higher in this non-standard cosmology. Computing the cumulative number density at different redshifts, we estimated that the expected number of massive clusters is enhanced in VDE by at least a factor of ~ 3 for the $M = 10^{15} \times h^{-1} M_{\odot}$ cluster and a factor of ~ 10 in the other two cases. Of course, these results might as well simply point in the direction of modifying the standard paradigm, for example including non-Gaussianities in the initial conditions or either using a higher σ_8 or Ω_M value for the Λ CDM as the comparison to the Λ CDM-vde model seems to suggest.

Nonetheless, this first results on the large scale clustering in the case of VDE cosmology point in the right direction, significantly enhancing the probability of producing extremely massive clusters at high redshift as recent observations seem to require.

ACKNOWLEDGEMENTS

EC is supported by the MareNostrum project funded by the Spanish Ministerio de Ciencia e Innovacion (MICINN) under grant no. AYA2009-13875-C03-02 and MultiDark Consolider project under grant CSD2009-00064. EC also acknowledges partial support from the European Union FP7 ITN INVISIBLES (Marie Curie Actions, PITN-GA-2011-289442). AK acknowledges support by the MICINN's Ramon y Cajal programme as well as the grants AYA 2009-13875-C03-02, AYA2009-12792-C03-03, CSD2009-00064, and CAM S2009/ESP-1496. JBJ is supported by the Ministerio de Educación under the postdoctoral contract EX2009-0305 and also wishes to acknowledge support from the Norwegian Research Council under the YGGDRASIL programme 2009-2010 and the NILS mobility project grant UCM-EEA-ABEL-03-2010. We also acknowledge support from MICINN (Spain) project numbers FIS 2008-01323, FPA 2008-00592 and CAM/UCM 910309.

REFERENCES

- Baldi M., Pettorino V., 2011, MNRAS, 412, L1
 Beltrán Jiménez J., Lazkoz R., Maroto A. L., 2009, Phys. Rev. D, 80, 023004
 Beltrán Jiménez J., Maroto A. L., 2008, Phys. Rev. D, 78, 063005
 Brodwin M., et al., 2010, ApJ, 721, 90
 Enqvist K., Hotchkiss S., Taanila O., 2011, JCAP, 4
 Foley R., et al., 2011, ApJ, 731, 86
 Gill S. P. D., Knebe A., Gibson B. K., 2004, MNRAS, 351, 399
 Hoyle B., Jimenez R., Verde L., 2011, Phys. Rev. D, 83, 103502
 Jee M., et al., 2009, ApJ, 704, 672
 Jenkins A., et al., 2001, MNRAS, 321, 372
 Knollmann S. R., Knebe A., 2009, ApJS, 182, 608
 Larson D., et al., 2011, ApJS, 192, 16
 Mortonson M. J., Hu W., Huterer D., 2011, Phys. Rev. D, 83, 023015
 Nesseris S., Perivolaropoulos L., 2007, JCAP, 0701, 018
 Prada F., Klypin A. A., Cuesta A. J., Betancort-Rijo J. E., Primack J., 2011, ArXiv e-prints
 Press W. H., Schechter P., 1974, ApJ, 187, 425
 Sheth R. K., Tormen G., 1999, MNRAS, 308, 119
 Springel V., 2005, MNRAS, 364, 1105

Tinker J., Kravtsov A. V., Klypin A., Abazajian K., Warren M.,
Yepes G., Gottlöber S., Holz D. E., 2008, ApJ, 688, 709

This paper has been typeset from a T_EX/L^AT_EX file prepared by the
author.